Running head: Plume Structure in a Wind Tunnel

Measurement of Odor-Plume Structure in a Wind Tunnel Using a Photoionization Detector and a Tracer Gas

Kristine A. Justus
Department of Entomology, University of California, Riverside

John Murlis
Department of Geography, University College London

Chris Jones
54 Sylvan Drive, North Baddesley, Hampshire, United Kingdom

Ring T. Cardé [1]
Department of Entomology, University of California, Riverside

[1] Corresponding author. Ring T. Cardé, Department of Entomology, University of California, Riverside, 92521 USA; email: ring.carde@ucr.edu; v: 909-787-4492; f: 909-787-3681.

Abstract. The patterns of stimulus available to moths flying along pheromone plumes in a 3-m-long wind tunnel were characterized using a high frequency photoionization detector in conjunction with an inert tracer gas. Four contrasting flow regimes and source conditions were produced: odor released in pulses from a vertical and horizontal array of four sources, odor released continuously from a point source, and odor released continuously from a point source into an oscillatory wake. Although the four flow regimes produced plumes of intermittent and fluctuating concentration, there were considerable differences in the structure of the signal presented to the sensor. Pulses of tracer gas released at 10 Hz retained most of their longitudinal and lateral separation. The plume growing in the disturbed flow ('oscillatory'), was broader in its lateral extent than the plume growing in an undisturbed flow ('continuous'), and the concentrations in the former were the lower at each downstream position. The signal recorded in the disturbed flow had higher intermittency, but the ratio between the peak concentration and the signal mean was lower than in the continuous plume. Time scales were typically longer in the tunnel than in a field setting, but length scales and the main features of intermittency and fluctuation were similar. Moths flying along plumes of pheromone in this and similar wind tunnels typically slow their velocity and narrow the lateral excursions of their flight track as they approach a pheromone source. Which features of the plumes measured in this study account for these behavioral reactions remains to be determined.

Keywords: insects, odor plume, orientation, pheromone, wind tunnel

Abbreviations:

$\langle C \rangle$ (with overbar) – conditional mean concentration

C_{source} – source concentration

C (with overbar) – mean concentration

c' – fluctuating component of concentration, C

$\hat{c}$ – instantaneous peak instantaneous peak concentration

EAG – electroantennogram

miniPID – miniature photoionization detector

SFC – stimulus flow controller

$TiCl_4$ – titanium tetrachloride

U – instantaneous streamwise velocity in the tunnel

U (with overbar) – mean streamwise velocity in the tunnel

u' – fluctuating component of U

V – lateral component of the instantaneous wind velocity in the tunnel

v' – fluctuating lateral component of velocity parallel to the wind tunnel floor

W – vertical component of the instantaneous wind velocity in the tunnel

w' – fluctuating vertical component of velocity perpendicular to the wind tunnel floor

γ – the probability of a non-zero signal

1. Introduction

Animals of many kinds use smell as a primary sense for locating resources such as food or mates. Odors from these resources are carried by wind or water in plumes in which the intensity of the odor is, in general, increasingly attenuated with increasing distance from the source. Observations, for example of smoke blown from fires, show that the distribution of material within such plumes is highly uneven, with a patchy and wispy form. Such fine-scale structure would be experienced by an ideal sensor as a signal of rapidly fluctuating intensity, and this has consequences even for natural olfactory sensors which may have lower frequency response.

The characteristics of odor plumes in wind tunnels have been shown to mediate the maneuvers of insects orienting upwind toward the source of odor [1, 2]. In particular, the fluctuating and intermittent nature of turbulent plumes of odor seems to provide information that insects use to set both their heading with respect to due upwind and their velocity along a flight track. In a classic series of experiments, Kennedy et al. [3, 4] showed that the upwind flight of male moths was arrested in either a well-mixed cloud of pheromone or in clean air, but that, upon re-entering the cloud, moths surged upwind. Similarly, it has been shown that female mosquitoes improve orientation along a plume of CO_2 if the internal structure of the plume is filamentous rather than homogeneous [5, 6].

There has been recent progress in the quantitative understanding of the dynamics of the interaction between plume structure and flight. For example, male moths flying along a plume of pheromone head more directly and rapidly upwind when they encounter filaments of pheromone at rates near 5 Hz; lower rates promote slower flight with wide zigzag maneuvers [1]. It is important, however, to recognize that in such upwind flight along odor plumes, the primary mechanism by which a flying insect sets direction and velocity, is an optomotor feedback system [7]. The insect detects wind flow by sensing how its position is modified relative to its visual surround. A generally front-to-rear image flow signifies a trajectory aligned with the wind flow, whereas flight direction relative to wind is presumably sensed by mechanoreceptor input. This suggests that the main role of the chemical makeup of the plume, including the intermittency and fluctuating form of the concentration signal it provides, is to maintain the optomotor response. To understand how this response is maintained and the optimum conditions required, experimenters have sought information on the instantaneous concentration of attractant in a plume and the concurrent movements of insects.

The considerable progress that has been made in understanding the fine-scale structure of dispersing plumes in the atmosphere [8, 9, 10 and 11] and in idealized wind tunnel conditions [12, 13] has clarified the broad features of concentration fluctuations and provided a set of analytical and

experimental tools. However, with respect to animal behavior, the link between cause and effect is not easily established. In work on insect orientation, it has proved difficult to correlate directly the fine-scale features of the plume with moment-to-moment behavioral maneuvers of experimental animals during flight along plumes in wind tunnels. Visualization of the plume, using titanium tetrachloride ($TiCl_4$) and video analysis (e.g., [14, 15]), allows the plume's overall boundaries to be established and provides some qualitative insight into the plume's internal structure. In an innovative approach, Vickers and Baker [16] and Vickers et al. [17] recorded electroantennograms (EAGs) from a flying moth. They mounted an excised antenna on the thorax of a male (dorsally between its antennae), and used a thin wire to carry the response to a conventional amplification system; this approach allowed monitoring of plume contact and therefore some direct comparisons of 'in-the-plume' and 'out-of-the plume' maneuvers.

There is also potential for producing stimulus patterns more akin to those found in the open atmosphere. A stimulus generator can be used to provide pulses of odor that simulate to some extent the filaments of a natural plume. Such pulse generators can be set to deliver odor pulses at rates up to 33 Hz with filaments of small size (ca. several cm diameter) and duration (e.g., 20 ms).

It will remain difficult, however, to carry out controlled trials of flight behavior in the open air, not least because plumes in the atmosphere are subject to large-scale changes in wind direction and velocity, particularly in complex environments. The objective of a wind tunnel is to model the physical environment whilst allowing for the experimental manipulation of one variable at a time [18]. To date, studies of insect orientation have used simple models to describe the stimulus an insect receives, based on time-averaged plume structure. This has limited the range of possible associations between stimulus and behavior. Insect orientation studies have typically used odor plumes that are generated from a point source, with or without a disturbance in flow (i.e., a continuous or oscillatory plume, respectively), and each of these elicit distinct patterns of flight (Fig. 1). Flight tracks tend to be straighter in the intermittent plumes produced by either an oscillatory wake or artificially by a pulsing apparatus, and flight tracks of insects given point source plumes tend to show a more zigzag pattern. However, the fine-scale structure of only one of these, the continuous plume, has been detailed [12, 13], and this leaves a gap in information available for relating behavior to plume structure. What would be useful is a system that would allow measurement of instantaneous odor flux in wind tunnels of the kind used for investigating insect flight behavior, over small cross-sectional areas at rates that are comparable to the reaction rates of the insects' chemosensory system.

In this paper we describe the use of a small (cross-sectional area 1 mm^2), high frequency (sampling rates up to 330 Hz), photoionization detector used in conjunction with an inert, passive, tracer gas. We have used this device to measure the characteristics of odor plumes used to study the flight of

male moths along pheromone plumes in a typical entomological wind tunnel. The immediate objective of our work is to compare the fine-scale features of odor plumes in the contrasting flow regimes that are typically used in insect behavior studies. Previous studies have examined changes in flight maneuvers as an insect approaches a source (for example, [19]). We have therefore chosen to study the region from immediately downstream of the source, to a maximum distance of 400 mm, in an effort to draw meaningful conclusions about changes in plume characteristics over a region of plume that, in terms of distances in the field, is close to the source. Our eventual aim is to understand how moment-to-moment contact with filaments of pheromone influences the moth's flight maneuvers.

The system we have developed is not optimized for the study of fluid mechanics of dispersing plumes but rather is a practical system to determine fine-scale features of airborne odor plumes that have been commonly used in insect investigations for several decades. In such highly complex arrangements optimized for the study of insect flight, there remains no substitute for an empirical approach in characterizing the stimulus that insects receive.

2. Materials and Methods

2.1 Wind Tunnel

The wind tunnel used in these trials was a typical insect flight tunnel similar to that used by Mafra-Neto and Cardé [1, 14, 15] and Cardé and Knols [20]. It was constructed from three sheets of 3 mm thick clear polyacrylic Lexan®. To make the tunnel, each sheet was bent into an arch-shape and connected to a 1-m-wide frame to create a symmetrical semi-cylinder 3-m in length with a center height of 1.5 m (Fig. 2). The floor was constructed from 10 mm thick clear Plexiglas® sheets. A push-pull airflow system was used with variable speed motors operating an upwind pusher fan and downwind exhaust fan.

Turbulence in the tunnel, as indicated by flow visualization, was greatly reduced by drawing air into the tunnel through a 150-mm-thick aluminum honeycomb, (Hexcel® 15 mm diameter cells), 200 mm downstream of the upstream fan. Two oblong openings were cut into one side of the tunnel, 270 mm from the upstream and downstream ends, to allow users access into the tunnel. Openings were covered with clear polyvinyl sheets so that airflow was not disturbed during recordings. Both ends of the tunnel were capped with 1 mm mesh screening. The tunnel was housed in a room with a controlled environment of 26-28 °C and 60-70% R.H. Wind speed in the tunnel during recordings was set at 500 mm s^{-1}.

The scale of turbulence in the tunnel was assessed using a 3-D sonic anemometer (CSAT3, Campbell Scientific, Utah). This instrument has a resolution of 1 mm s^{-1} root mean square (rms). Orthogonal wind components U, V, and W, where U is the instantaneous streamwise velocity measured along the wind tunnel, V is the instantaneous lateral component of velocity parallel to the wind tunnel floor, and W is the instantaneous vertical component of velocity, were sampled at 60 Hz at five positions along the tunnel's centerline ~230 mm above the floor (the height of the plume during anemometer measurements, and the minimum height that could be sampled due to the dimensions of the anemometer). Digital outputs were recorded on a laptop computer. Mean streamwise velocities and the intensities of velocity fluctuations were determined for all four plume types (Fig. 3).

2.2 Plume Generation

The tracer used in these trials to simulate odor was a mixture of propene and air. For all plume types, a 1000 ppm propene in air mixture was delivered to a stimulus flow controller (SFC-2; Syntech, The Netherlands). The gas mixture from outlets on the SFC-2 was then introduced into the wind tunnel via one or four Pasteur pipettes inserted through the floor of the tunnel, at a flow rate of 2.5 ml s^{-1}. When one pipette was used, gas from one outlet was injected via the pipette at a rate of 2.5 ml s^{-1}; when four pipettes were used, the effluent was split from two outlets (Fig. 4a), resulting in flow rates of 1.25 ml s^{-1} from each pipette, pulsed simultaneously for a total of 5 ml s^{-1}. Each pulse from a pipette contained the equivalent of approx. 0.25 µl of propene (250 µl of 1000 ppm propene mixture). Velocity of tracer gas released as a continuous stream was approximately 800 mm s^{-1}; pulsed plume release velocity was isokinetic with the tunnel wind speed.

The tip of each pipette was bent at ~ 45 ° prior to use (see [21]) and positioned so that the aperture faced upstream (Fig. 4b) with the tip at a height of 180 mm above the floor. A single pipette was used to produce a continuous point source plumes and a continuous point source released into an oscillatory wake. For the oscillatory plume, a circular disk (35 mm diameter) was placed approximately 25 mm downstream of the pipette and perpendicular to the flow (Fig. 4c). Two configurations of pulsed plumes were generated from a four-pipette linear array: a horizontal arrangement to create a broad plume and a vertical arrangement to create a tall plume. Such arrangements are used in wind tunnel trials [21] to generate larger cross-sectional plumes because flight tracks of moths vary spatially in both horizontal and vertical planes. In each case, pipettes were set symmetrically about the centerline of the tunnel in a wire mesh (6 mm) holder so that pipette outlets were spaced at approximately 1.8 cm.

We recorded signals from four types of plume:

1. Pulsed horizontal line source (hereafter called the 'horizontal plume'): plumes emanating from a horizontal rake of four pipettes placed symmetrically about the tunnel center line with the output from the pulse generator configured to 20 ms pulses at 10 pulses s^{-1}.
2. Pulsed vertical line source (hereafter called the 'vertical plume'): plumes emanating from a vertical rake of four pipettes placed symmetrically about the tunnel center line with the output from the pulse generator configured to 20 ms pulses at 10 pulses s^{-1}.
3. Continuous point source release (hereafter called the 'continuous plume'): a plume from a single pipette developing in the flow of the wind tunnel.
4. Continuous point source release into an oscillatory wake (hereafter called the 'oscillatory plume'): a plume issuing from a single pipette with a circular disk downstream of the source, as described above and shown in Fig. 4c.

2.3 Plume Detection and Analysis

The sensor used was a fast-response, miniature photoionization detector (miniPID; Aurora Scientific, Canada) with a frequency response rate of 330 Hz and a detection threshold of 50 ppb propene. The sensor was mounted on a computer-controlled traverse with movement in the longitudinal (x-), horizontal (y-), and vertical (z-) axes. This allowed us to place the miniPID within the wind tunnel with a precision of 0.25 mm. The arrangement of connections to the sensor head limited the portion of the tunnel over which measurements could be taken to a region of approximately one quarter of its cross-section. The sampling rate of the miniPID was 18.3 ml s^{-1} through a 1 mm^2 cross-section inlet. The miniPID controller has three gain settings (1, 5, and 25) and a potentiometer for adjusting the baseline signal level (i.e. the electrical signal produced by the equipment in absence of a tracer gas.) Noise measured from the probe running in the tunnel without tracer gas was found to be less than 10 mV rms at the medium gain setting, equivalent to less than 0.25 ppm.

Symmetry about the longitudinal axis of the plume was confirmed initially by observation of a $TiCl_4$ 'smoke' plume. For all plume types, the output signal from the sensor was recorded within the upper portion of one half the cross section of the plume; that is, from center outward in both the horizontal and vertical directions. Measurements were taken at 50, 100, 200, and 400 mm from the (upstream-turned) tip of the pipette. This region near the source is of particular importance because it is within this range that a moth appears to alter its flight behavior as it approaches the odor source [19, 22,

23]. Recordings of 15 s duration were made every 3 mm along the vertical and horizontal axes within the cross section. The record length was chosen to give convergence of signal characteristics with manageable file size. Short record lengths may compromise the representation of very low signal frequencies. In this case, the record length is about seven times the period of the lowest frequency peaks shown in the spectral analysis (see below). The regression of concentration fluctuation intensity onto mean concentration, using data from the plume core, showed a low variance about the regression line, suggesting that the sampling system produces convergence of intensity within the ensemble. Recordings that were essentially zero (i.e., no tracer registered by the sensor) were excluded from analyses. Care was taken to record 'blank runs' every 10-20 recordings to acquire an accurate baseline; this was especially important with the continuous plume because, in many instances, the miniPID signal did not contain patches of zero to provide an internal baseline.

The analog voltage signals from the miniPID were digitized and logged on a computer using a specially developed Data Acquisition system (GemAcq-4; Gemini Enterprises, UK). The sampling frequency was set at 100 Hz (sufficiently high to resolve structure perceived by a moth's central nervous system, which has maximum frequency responses of the order of 10 Hz [17, 24]) and the full voltage span of 5 V was digitized at 12 bit resolution. This provided satisfactory signal-to-electronic-noise ratios under all operating conditions. Data then were converted from voltages to equivalent concentrations using a routine in the GemAcq-4 software. In subsequent statistical analyses (see below), a discrimination threshold of 1 ppm propene (determined by inspection of recordings) was used to reject noise (equivalent to approximately four times the rms noise).

The plume structure was averaged over an area (12 by 12 mm) matched to the typical physical dimensions of the sensory systems of male moths used in flight tunnels. (*C. cautella* antennae are 5 mm in length and held in front of the head while flying so that the maximum distance between left and right tips is ~ 4 mm.) Statistics were calculated using up to 25 recordings made within a 12 by 12 mm cross-sectional area (at 3 mm intervals) along each plume's axis at specific distances downstream. Some records were rejected because of external noise or sensor malfunctions. The number of usable recordings in an ensemble varied from 16-25, with most ensembles consisting of 20-25. Analyses of variance (ANOVAs) were run on these parameters for both within plumes at various distances from source, and among plume types. The principal characteristics measured for each 15 s sample of the sensor signal were as follows:

- Mean concentration (calculated from an ensemble of 16-25 recordings taken at the axial 12 mm by 12 mm center of the plume) and a measure of its fluctuation (standard deviation);

- Intermittency (defined here as the probability of zero signal, $1 - \gamma$, the proportion of time for which concentration was below the noise threshold, following the convention of Murlis and Jones [8] and Jones [9]. With this definition, zero intermittency is associated with a continuous signal, increasing intermittency is linked to less overall signal activity which is intuitive. Note that many authors use a different convention, defining intermittency as, γ, the probability of non-zero signal.);
- Peak-to-mean ratio;
- Peak-to-conditional-mean ratio (Conditional averages are those formed from ensembles of data taken when signal is present, see for example Mylne and Mason [10].);
- Mean length of bursts (Bursts are defined as periods of active signal above threshold, as in Murlis and Jones [8].).

Further analyses of the frequency content of the miniPID signals were made as follows. Replicates were exported as a numerical sequence to a statistical package (Statistica 5.0, StatSoft Inc., Oklahoma) and analyzed with the Spectral Frequency Analysis option (Single Series Fourier Analysis). This procedure subtracts the mean and detrends the input data before applying the Fast Fourier Transforms algorithm to convert the time series into a frequency spectrum that can be plotted as a periodogram or as a Spectral Density plot. Spectral Density estimates are computed by smoothing the periodogram values with a weighted moving average. This transformation improves the clarity of the frequency regions (consisting of several adjacent frequencies) that contribute most to the overall periodic behavior of the series. In this case, Spectral Density estimates were calculated using the Hamming weights with a window width of 5 values (0.0357, 0.2411, 0.4464, 0.02411, and 0.0357).

3. Results

3.1 Tunnel Wind Speeds and Turbulence

The mean tunnel speeds, measured by the sonic anemometer are shown in Fig. 3a. The tunnel speed fell slightly (about 10%) along the tunnel for all configurations, suggesting a hindrance in the exhaust system. The effect of the circular disk (in the oscillatory plume) was to add a velocity anomaly at the first measuring position (50 mm), but the tunnel's wind speed had recovered by the third position (100 mm). There was a range of speeds in the different runs, equivalent to about (±) 10% in the worst case.

Turbulence intensities were calculated as the square root of the mean of the squared fluctuation about the mean velocity in the case of the streamwise component, or the square root of the mean of the squared values of the fluctuating velocities in the case of the cross-flow components, and referenced to the streamwise mean (the tunnel wind speed). Generally, turbulence intensities were in the range 1% to 10% of the streamwise mean. Streamwise fluctuations and lateral fluctuations were of similar magnitude, but the vertical component fluctuations were about 50% of this level. The disk clearly increased turbulence levels, particularly in the forward region of the tunnel to a range of 10% to 30% of the streamwise mean. All components of turbulence increased toward the outlet end of the tunnel. This may also be a result of the configuration of the exhaust system.

3.2 Plume Forms and Dimensions

Flow visualization, using $TiCl_4$, showed the general form of the plume types. The continuous plume started as a jet with initial mixing at the source and much fine structure. It expanded slowly downstream. The oscillatory plume grew more rapidly and contained more identifiable large-scale structure, dominated by vortex shedding from the disk.

There are several possible criteria for defining the plume edge. Here we define the edge as the boundary at an intermittency value of > 0.9, and use this as a measure of the plume diameter. Assuming symmetry, the continuous plume grows from a diameter of roughly 30 mm to 40 mm between 50 and 200 mm downstream and the oscillatory plume from 60 mm to 90 mm over the same distance. Over this portion of the tunnel it seems that the horizontally pulsed plumes retain lateral separation and it appears that the lateral extent of the pulses changes very little as they progress downstream. However, these pulses appear to expand in the vertical plane as they progress toward the end of the tunnel. In the vertical array, there seems to be greater merging between pulses, although the cores remain distinct at least to 200 mm downstream of the source.

3.3 Concentrations and Their Distributions

Typical concentration traces are shown in Figs. 5, 6, and 7 for pulsed, oscillatory, and continuous plumes, respectively The signal appears as a series of pulses of varying amplitude separated by periods of zero amplitude. They show fluctuating concentration and intermittency and a decline in concentration

with distance from the source. Because the total flux of material across a given plane perpendicular to flow on average must be constant, an increase in plume size results in a concomitant reduction in mean concentration locally within that plane. Hence as a general rule we would expect to observe, for a given air stream velocity, turbulence regime, and release rate, a progressive reduction in local mean concentration as the distance downstream increases. However, as shown, for example in Murlis et al. [25], there are differences in the rate at which the different measures of concentration change with downstream distance (see 3.5 below). This has the consequence, for example, that peak concentrations may decrease less rapidly than mean concentrations, giving the peak levels in a signal increasing significance at greater distances from source Murlis et al. [25].

Mean and conditional mean concentrations measured within the 12 mm by 12 mm core region of the row of pulsed plumes, both from the vertical and horizontal rakes, are significantly lower ($P < 0.05$) at 400 mm from source than at 50 mm (Fig. 8 shows the conditional mean). Similarly, mean concentrations taken from the 12 mm by 12 mm core of the continuous and oscillatory plumes decline as distance from the source increases with measurements at 50, 100 and 200 mm significantly different ($P < 0.05$), but there is no significant difference between mean concentrations at 200 mm and 400 mm. The concentrations at 200 and 400 mm are approximately 20% of the concentration 50 mm from source.

The standard deviation of the fluctuating component of the concentration signal is a measure of the 'intensity' of the concentration fluctuations and is shown here as a ratio to the local mean concentration. We have estimated this ratio for each 'x' position by plotting the standard deviation of the fluctuating concentration against the mean taken from each of the records for each of the (12 by 12 mm) cross sections and calculating the slope of a linearized approximation to the relationships. This enabled us to combine data from across the whole core regions of the plumes.

In the pulsed plumes, intensities are 1.5 - 2 times the mean, regardless of distance from source. However, in both the continuous and the oscillatory plumes, the ratio increases downstream, with values more than doubling from nearest the source to 200 mm downstream (Fig. 9). This may be due in part to large decreases in mean concentration of these two plume types as they travel downstream (Fig. 8). Fackrell and Robins [12] also found that relative intensity of fluctuations increased with distance in a region close to the source, up to about 2.4 meters downstream, equivalent to about 300 mm in our flow.

The values we derived for the intensity of concentration fluctuations compare well with the values obtained by Mylne and Mason [10] in the field during neutral conditions of atmospheric stability and with those of Fackrell and Robins [12, 13] in the laboratory. We find intensities of about 2 and 1.5, respectively, for the horizontally- and vertically-aligned arrays of pulsed plumes and ranges of 1.2 to 2.0 and 0.5 to 1.2 for the continuous and oscillatory plumes. Mylne and Mason found that intensity fell

rapidly in the initial region close to the source, but approximately constant intensities in the range of 0.5 to 2.0 in the region further from the source. In their wind tunnel experiments, Fackrell and Robins obtained values in the range 2.0 to 0.8, decreasing with increasing distance from the source in the region beyond about 2.4 meters (equivalent to about 300 mm in our flow). It is not clear to us, however, why the intensity increased toward the end of the tunnel in the continuous and oscillatory plumes. We note that this is a region in which turbulence intensity also increases whereas mean streamwise velocity falls (Fig. 3a), so that this, too, may be due to blocking effects in the tunnel exhaust system.

Skewness and kurtosis close to the plume axis are close to the values expected for a normal Gaussian distribution, zero and 4 respectively. However, at the edges of the plume distributions become leptokurtic and skewed toward higher values (Fig. 10).

3.4 INTERMITTENCY

Intermittency in the axial center of continuous and oscillatory plumes is low, but greater than zero, and increases toward the plume edge (Fig. 11). The across-plume profiles vary with distance downstream. Close to the source, the profile tends to be flat with a large core of intermittency values near zero, which then increases toward the plume edge to values near 1.0. However, downstream the profile shows a systematic increase in intermittency from the axis to the edge.

Moreover, for all the plumes, the measured intermittency at the centerline increased with distance from the source (Fig. 12). The continuous and oscillatory plumes showed systematic increases with distance downstream, but the continuous plume's centerline intermittency reaches its peak at 200 mm. The largest changes in intermittency with consecutive downstream distances were observed in the oscillatory plume. For the pulsed plumes, however, the increase was not evident until 400 mm from the source. For both continuous and oscillatory plumes the intermittency seems to plateau at about 0.6 at 200 mm downstream of the source. This is lower than the values found by Murlis and Jones [8] and Jones [9] in field measurements, which are about 0.8 at a roughly equivalent distance, but within the range of values (0.4 to 0.8) in wind tunnel measurements of Fackrell and Robins [12]. The field measurements can be expected to give higher intermittency due to the effects of undulation and meandering. Fackrell and Robins found a very significant effect of source size on intermittency: our measurements compare well with their measurements from a source of approximately 15 mm. Fackrell and Robins used a wind tunnel speed of 4 m s^{-1} but even so, their results suggest that that our effective source size may not be well characterized by a value based on the bore of the pipettes (1 mm).

3.5 Peak-to-Conditional-Mean Ratios

One of the main characteristics of a fluctuating signal is that there is a considerable contrast between peak amplitudes and the mean. In these concentration signals, the peak-to-mean ratio has been estimated as a ratio of the highest value registered in a sample to the overall sample mean and, to eliminate the influence of intermittency, to the conditional mean. Peak-to-mean and peak-to-conditional-mean ratios were similar, but because the overall means of the pulsed plumes are dominated by intermittency due to pulsing, only the peak-to-conditional-mean ratios can be interpreted. Measured peak-to-conditional-mean ratios averaged over an ensemble of samples from the 12 mm by 12 mm core of each plume type are shown in Fig. 13. Peak-to-conditional-mean ratios for the continuous plume show no significant trend with distance from the source at values of approximately 4.2. For the oscillatory plume, ratios are significantly lower ($P < 0.05$) furthest downstream with no significant differences at distances of 50, 100, and 200 mm from the source with values of about 4. The corresponding peak concentration to overall mean concentration ratios, which is about 10 to 15, are lower than values reported in field trials [8, 9, 25] which are in the range 20 to 30 and this could be due to the impacts of meandering and undulation on the overall mean. In both these cases, the peak to conditional mean ratios fell less steeply with downstream distance than conditional mean, suggesting that peaks in the signal become less marked closer to the source. In both vertical and horizontal plumes, ratios were significantly greater ($P < 0.05$) nearest the source than at 400 mm downstream, but each showed different patterns. Peak to mean ratios in the horizontal plume declined systematically from approximately 7, leveling off at 200 mm downstream at about 3.5, whereas the vertical plume at 100 and 200 mm downstream shows similar intermediate ratios of about 3.8. The ratios of the continuous and oscillatory plumes close to source differ from those of the pulsed plumes, and it is possible that the higher peak to conditional mean ratios in the pulsed plumes arise from deviations in the form of the pulses from the ideal "square waveform".

3.6 Burst Lengths

Intermittency is a useful measure of the average time-dependant structure of a signal, but loses the details of the fine-scale structure. A signal of a given intermittency could be comprised of a few long, well-separated bursts or of many closely packed bursts. The burst length is of biological interest because many odor sensors adapt when exposed to a stimulus for any length of time (see [26] for a discussion of adaptation).

On the plume edge where the signal is highly intermittent (that is, there are significant periods when the concentration is less than 1 ppm), we generally expect to see the shortest burst lengths and the highest mean interval between bursts. Correspondingly, the total number of burst events will diminish toward the plume edge as fewer and fewer peaks in the signal achieve levels above the threshold. A rather different type of behavior is displayed on the plume axis where there are few occasions when the signal falls below the discrimination threshold and only a small variation in concentration occurs over the entire record.

During these trials, pulses generated were 20 ms in duration. However, the measured burst lengths suggested that the pulses produced contained internal structure with bursts of shorter lengths, which expanded initially as they moved down the tunnel before diminishing downstream (Fig. 14a). The burst lengths in the continuous plume were significantly greater ($P < 0.05$) at 50 mm from the source (about 2 seconds) than at 200 and 400 mm from the source (about 0.5 seconds) and, although not significant, a similar trend in the oscillatory plume was observed with burst lengths in a range 0.3 to 0.7 seconds (Fig. 14b). These mean burst lengths are long compared to those measured in the field [8, 9], which are of the order of 0.2 seconds. However, the field measurments are heavily influenced by large-scale movements of the plume. In terms of length scale, there is closer agreement with tunnel bursts associated with length scales of 150 - 350 mm and bursts in the field with mean lengths of about 400 mm.

3.7 Frequency Spectrum of Concentration Fluctuations

The Fourier analysis of the pulsed plume signal was dominated by the pulse emission rate of 10 Hz (Fig. 15)]. For the continuous and oscillatory plumes, however, spectral density plots show a more widely distributed spectrum with strong contributions from frequencies below 5 Hz, particularly closer to the source (Fig. 15). The corresponding periods for the spectral peaks, 200 ms at 5 Hz and 100 ms at 10 Hz, are large compared to the burst lengths measured, which are tens of ms in length. Moreover, the dominant frequencies in the spectrum change with position along the tunnel. For example, Fourier analysis of the oscillatory plume at 100 mm from the source shows strong peaks at 0.4, 1.9, and 3.2 (Fig. 15d) but at 400 mm downstream from the source, peaks are observed at 1.0, 3.7, 4.1, and 5.2 (Fig. 15e).

In these trials a circular paper disk was used to generate turbulence. Air spilling over the disk in an arrangement of this kind produces a series of vortices shed from alternate sides of the disk with a characteristic frequency. The non-dimensional form of this frequency is the Strouhal number (see for example, Vogel [27]), calculated as $St = nl/U$, where n is the frequency of the periodically varying flow,

l is a transverse dimension, and U is the fluid velocity. In the case of our oscillatory plume at 100 mm downstream from the source, there are strong frequency contents at 1.9 Hz and 3.2 Hz, giving St = 0.133 and 0.224, respectively. These values are typical of those found respectively for long flat plates and circular cylinders set laterally to the flow.

4. Discussion

The principal motivation for these trials was the need to characterize the stimulus available to insects flying along airborne odor plumes. The ultimate aim was to measure the structure of surrogate odor plumes in a wind tunnel so that the principal features could be related to behavioral maneuvers of male moths flying along pheromone plumes of the same form. This would provide a working guide for future studies and a means of interpreting differences in behavior seen in previous work. Although there is an abundance of laboratory studies of insect navigation, to date, relatively little work has been reported on the structure of the air-borne plumes along which these insects orient, other than time-averaged, plume boundaries. Therefore, interpretations of behavior have been based mainly on output (i.e., flight characteristics) rather than input-output (i.e., what instantaneous signal is intercepted by the animal and the resultant flight patterns).

Previous studies have shown demonstrable effects of plume structure on the flight path of moths. Mafra-Neto and Cardé [1] reported flight tracks (mean track angles of 41.5° ± 12.1) more toward upwind (0°) in a turbulent plume (similar to the oscillatory plume presented here) and plumes pulsed at 5 per second produced similar flight tracks (mean track angles of 40.4° ±14.0). However, slowly pulsed plumes of < 1 per second produced flight tracks with more crosswind headings (73.9° ±7.2). Similarly, male gypsy moths produced tracks of slower ground speed and greater track angles in plumes from a point source compared with a more diffuse plume from a cylindrical baffle [28]. Furthermore, flight behaviors, such as ground speed and track angle, change as an insect approaches an odor source [19, 22, 23], suggesting that plume characteristics evoke specific behaviors and that changes in plume characteristics induce alterations in flight behaviors.

A further problem is that of replicating in laboratory conditions the pattern of odor stimulus and wind found in the field and described in, for example, Murlis and Jones, [8] and Murlis et al. [25]. The main difference between the conditions in the laboratory and the field is that, in wind tunnels, the scale of turbulence is severely constrained so that the plume neither meanders nor undulates and the intensity of

large-scale fluctuations in wind speed is considerably diminished. The magnitude of concentration of the chemical stimulus in these wind tunnel trials is designed to be of a similar level to that found in the field and the intensity of fluctuations appears not to be enormously different from the levels described in the field by Mylne and Mason [10]. The mechanical forces acting on the flying insect, however, due to turbulent fluctuations in wind speed and direction, are far less in wind tunnels.

For more than 50 years, flight tunnels of the kind we describe, have been used in entomological investigations of the behavioral roles of particular odorants, response profiles to individual components or ratios of blends, sensory adaptation, habituation, and disruption, and mechanisms of orientation (see [18]). Laboratory flight tunnels are generally rectangular or arch-shaped in cross-section and rarely longer than 2 m. The ends of the tunnel are usually capped with window screening or cheesecloth to contain flying insects and, at the upstream end, to reduce the level of turbulence in the airflow. Characterizing the flow has typically been through the use of visual markers, such as cigarette or $TiCl_4$ 'smoke'. Although these markers are useful to define roughly the time-averaged boundaries of a plume and to give a qualitative understanding of structure, they are not strictly passive and it is difficult to make quantitative measures of plume structure using them. To date, instantaneous plume structures of pheromone plumes have not been described in sufficient detail to allow comparison with the subtle changes seen in the flight maneuvers of insects. In particular, differences in the fine-scale features of the plume near the source where the flow is not fully developed, have not been explored, although changes in flight behaviors in this region have been observed in insect studies [19, 22, 23]. In this paper we describe the differences in the forms of signals taken from plumes in their initial stages in these flow regimes and suggest ways in which these signals could modulate the insect's flight response. The results reflect the real conditions in which flight trials are carried out in laboratories, and we believe that this analysis provides insights into the signals insects typically encounter in work of this kind.

Usually, the plumes used in entomological studies are generated from a pulsing apparatus (pulsed plume), a point source such as a filter paper impregnated with a volatile odorant (continuous plume), or a continuous plume source with a disturbance in flow (oscillatory plume), and each of these elicit distinct patterns of flight (Fig. 1). Flight tracks in pulsed and oscillatory plumes tend to be straighter than flight tracks in continuous plumes. Flight tracks in pulsed plumes can resemble more closely either those in continuous or oscillatory plumes, depending on the pulsing rate (crosswind flight occurs at low pulse rates) and plume diameter (animals tend to exit small diameter plumes frequently). Here, we have measured the fine-scale features of each of these plume types and note that certain features are distinctly different in the different plume types. For example, absolute average concentrations in the plume centerline are three to five times higher in the continuous plume than either of our pulsed plumes, and

oscillatory plumes about half that of the continuous plumes. Mean burst lengths follow a similar pattern with the continuous plume showing longer bursts, at least near the source, and the oscillatory plume producing short bursts similar to the pulsed plumes.

There are three plume properties that vary systematically with distance from source during the initial stages of plume development and which may play a role in mediating the flight behaviors of insects as they approach a source. They are mean concentration, intermittency, and in the case of continuous and oscillatory plumes, intensity of concentration fluctuation. There may be other features of the plume that play a role in orientation.

In each of the flow regimes the signal is intermittent and fluctuates in strength. Where the tracer source is pulsed, artificially introduced intermittency dominates over the length of the plume. In this case the pulse length, initially 20 ms, matches typical burst lengths measured in the field [25]. In addition, the periods of inactive signal of the continuous and oscillatory plumes were broadly within the ranges of burst return periods found in intense periods of bursts measured in the field, although they did not vary as much as would be the case in the field [25]. An inspection of the signal in the continuous plume (Fig. 7) suggests that a fixed sensor in it would register greater intermittency than it would in the oscillatory plume (Fig. 6), with fewer bursts and shorter burst lengths and correspondingly shorter intervals between bursts. The plume width, about 30 mm, was of a sufficient scale to engulf insects of the species typically used in the flight trials. However, insects often carry out counterturning maneuvers yielding a zigzag flight path, which can readily take them outside of the time-average boundaries of the plume. Such lateral excursions would affect their perception of intermittency and flux in the signal they encounter.

In flight trials, the number of excursions made by male almond moths, *Cadra cautella*, across the centerline of a pheromone plume was 3-5 per second [14], and that of male gypsy moths, *Lymantria dispar*, was 3-4 per second [20]. Furthermore, an animal maneuvering along a plume's edge alters its perception of the plume such that it encounters a fluctuating signal. Edge-following behaviors have been observed in the moths *Adoxophyes orana* [3, 4], and *Grapholita molesta* [29], and in the blue crab, *Callinectes sapidus* [30], and the copepod, *Temora longicornis* [31]. Following an edge or boundary provides an animal with a series of on-off signals. In these cases where the animal exits the boundaries of the plume, perceived intermittency would be higher than the actual intermittency in the plume; that is, less time is spent in signal above threshold. Whether or not an insect maintains a due upwind heading or zigzags off the wind-line, alters potential, real-time actuation by its receptors. The intermittency recorded by a stationary sensor within the plume, therefore, underestimates the realized intermittency of a moving insect counterturning upwind *through* the plume. The oscillatory plume described here is roughly twice the diameter of the continuous plume and grows more rapidly as it advances downstream. At this size,

the plume would engulf the insects, during all but the most extreme lateral movements. The well-mixed internal structure of this plume contains slightly shorter burst lengths and lower intermittency but large differences in concentration compared to the continuous plume. Such a plume is likely to provide a signal with a more constant stimulus and a lower mean concentration, a consequence of which could be sensory cell adaptation.

We have treated estimates of intermittency with caution because intermittency is dependent on the discrimination threshold set. As threshold increases, intermittency values will become large, eventually reaching a value of 1, where the threshold exceeds the peaks of odor bursts in the signal. In these trials, the threshold is fixed, but in the case of a biological sensor (i.e., a flying moth), threshold will vary with adaptation events (where threshold increases) and with either disadaptation or sensitization events (where threshold decreases).

Similarly burst length is dependent on threshold set; burst lengths decrease as threshold increases. With our static sensor and a threshold of 1 ppm, burst lengths of the continuous plume decreased with distance from source. Such relative changes that correlate to distance from source may influence the flight track of a moth orienting along such a plume, and changes in flight behaviors of moths approaching a source have been reported. For example, Willis et al. [32] found that flight tracks of gypsy moths were narrower and ground speeds decreased closer to a point source in the field. An insect that flies rapidly through long bursts and slower through short bursts, encounters a less variable burst length, but its experience of the rate of onset of that signal is also altered.

Another feature of the odor signal that has been proposed as a behavioral cue, is the rapid rise in concentration at the leading edge of bursts. Atema [33] noted systematic changes with distance from source in the rate of rise in concentration at the leading edge of bursts and suggested that this formed part of the information used by lobsters, *Homarus americanus*, walking up a flume to a source of food odor. This is an explicitly chemotactic mechanism. It does not rely on rheotaxis, orientation to the direction of current flow, but instead, depends directly on changes in the physical structure of the plume, in this case, the rise in concentration at the leading edge of bursts, to regulate upstream maneuvers. Whether flying moths use the rapid rise in concentration at the leading edge of bursts is currently unknown. Webster and Weissburg [34] found that blue crabs did not appear to have the ability to resolve the slope a leading edge of a concentration burst. Bursts observed in recordings by our stationary miniPID (e.g. Figs. 5, 6, and 7) show very rapid burst activity with steeply sloped leading and trailing edges. It seems unlikely that moths would have ability to resolve these temporal characteristics, given that response rates of projection neurons in the central nervous system of those moths studied seem to be limited to 10 Hz or so [17, 24]

Over the range of source-to-sensor distances examined in this study, peak-to-conditional-mean ratios decrease with distance from the source in pulsed plumes, are unchanged in the continuous plume, and show no trend in the oscillatory plume. Interestingly, a plume type that is used often in insect orientation studies – a 'turbulent plume' within a laminar flow, (e.g. [14, 35]), described here as an oscillatory plume – is also the plume type that shows no trend in peak-to-conditional mean ratios with downstream distance from source. The variability of this parameter suggests that it is not a reliable one for predicting distance to source. Furthermore, as we have stated for steeply sloped edges of bursts, moths appear to possess a neuronal resolution an order of magnitude lower than would be required to sufficiently resolve peak-to-conditional mean ratios. Therefore, peak-to-mean ratios are not likely to be involved in orientation of flying moths.

Although Fourier analysis unveiled some periodicities of low frequency in the continuous and oscillatory plumes, it seems unlikely that the periodic nature of the signal *per se* is important to a male moth orienting along a pheromone plume but rather the presence of a sufficient number of filaments per second presented to the insect ensures that the animal continues upwind progress rather than 'casting' without progressing upwind [1, 14, 15]. Periodicities of the oscillatory and continuous plumes changed with tunnel position, exhibiting larger frequencies further from the source. In fact, the rate of interception of pulses has a considerable influence on flight maneuvers. *Cadra cautella* flies faster and more toward upwind in pulsed plumes of $\geq$10 Hz than in plumes pulsed at $\leq$ 5Hz [15, 21]. The changes exhibited in these maneuvers as an insect approaches a source, such as a decrease in flight speed [32], could be due to these changes in the plume's periodicity. Periodicity of concentration fluctuations in oscillatory plumes in flight tunnels has not previously been described.

The present measurements made in the kinds of plume types routinely employed in studies of moth orientation to pheromone ([21], *et ante*) confirm that structural features of these plume types differ, and that these features change systematically within 100 to 400 mm of the upstream sources of odor. These characteristics are candidate cues for the observed changes in flight maneuvers as male moths approach pheromone sources. Among the behavioral changes typically observed are a decrease in velocity along the track and a narrowing of the track's lateral extent [19, 22, 23, 32]. Such changes are often a prelude to landing near (or sometimes on) the odor source. Because of intermingling effects of dynamic thresholds, sensory cell adaptation, counterturning in freely-flying animals, and temporal scales of resolution unique to biological systems, we suggest that the rate in rise of concentration at the leading edge of bursts, peak-to-mean ratios, and periodicity are not used by male moths in locating pheromone sources. In addition, we suggest that intermittency is not used by male moths to distinguish 'near' or 'far' from a plume's source, but rather that an intermittent plume is required to sustain upwind progress. We

suggest that the flight track is shaped by a combination of absolute concentration and burst length, and that as a moth approaches a source, concurrent changes in concentration and filament interception rate may induce changes in flight behaviors.

5. Acknowledgement

We thank Drs. E.A. Cowen and M.J. Weissburg, and two anonymous reviewers, for helpful comments on this manuscript. We are grateful to Dr. J. Bau for performing Fourier analyses, and to Mr. D. Giles and Mr. P. Stovall, College of Engineering at the University of California, Riverside, for the design and fabrication of the x,y,z-traverse,. The research was supported by a grant from the Office of Naval Research (ONR N00014-98-1-0820) under the ONR/DARPA Chemical Plume Tracing Program.

Fig. 1. Flight tracks of male *Cadra cautella* in three different plume types. Flight tracks displayed are in a region approximately 200-700 mm from the source. Pulsed plume: generated by an electronic pulsing apparatus and introduced to the wind tunnel through a horizontal rake of four pipettes, each containing a pheromone-laden filter paper disk, release velocity was isokinetic with wind tunnel airflow (see [21]). Continuous plume: issuing from four pipettes, each containing pheromone-laden filter paper disk, and a continuous airflow of 2.5 mL s^{-1}, released as a jet (see [21]). Oscillatory plume: issuing from a pheromone-impregnated filter paper disk mounted on a copper wire with a 30 by 30 mm plastic deflector 40 mm downstream of the filter paper disk (see [14], reproduced with permission). Tick marks on the abscissa are each 100 mm. Each dot represents the position of the moth every other frame: 0.067 s for tracks in the pulsed and continuous plume; 0.033 s for the track in the turbulent plume. Track angles and airspeeds reported are means of all flight tracks of animals in those conditions. (See [21] for behavior of moths in pulsed and continuous plumes; see [14] for behavior of moths in oscillatory plumes.)

Fig. 2. A 3-m long wind tunnel typical of entomological studies, constructed with Lexan® and Plexiglas®. The upwind end has a 150-mm deep block of aluminum Hexcel® to laminize airflow. Window screening covers both the upwind (not shown) and downwind ends of the tunnel. A cowling of polyvinyl sheeting attaches the downwind end to an exhaust duct (not shown). Openings in the side of the tunnel are sealed with polyvinyl sheeting to minimize the disturbance in airflow during experiments.

Fig. 3. Orthogonal wind components, U, V, and W, in a wind tunnel sampled at 60 Hz with a 3-D sonic anemometer. (a) wind speed in the tunnel, (b) intensity of fluctuations in the streamwise velocity, (c) intensity of fluctuations in the lateral component of velocity parallel to the wind tunnel floor, and (d) intensity of fluctuations in the vertical component of velocity.

Fig. 4. Odor sources issuing from modified Pasteur pipettes. (a) A linear array of four pipettes (not drawn to scale) were set ~18 mm apart. Airflow (2.5 ml s^{-1}) from each of two pulse generator outlets was split to two pipettes via polyvinyl tubing; (b) the linear array was set either horizontally, as shown, or vertically; arrow denotes wind direction in the flight tunnel; (c) a continuous point source released into an oscillatory flow was produced by placing a 35 mm circular paper disk (shown as a black line) ~ 25 mm upstream of a modified Pasteur pipette via copper wire (shown as gray line); arrow denotes wind direction in the flight tunnel.

Fig. 5. Representative traces at the axial center of one of the odor sources of the vertical pulsed plume using a miniature photoionization detector (miniPID) at four distances downstream of the odor source: (a) 50 mm, (b) 100 mm, (c) 200 mm and (d) 400 mm. Each trace is 15 s.

Fig. 6. Representative traces from the axial center of the oscillatory plume using a miniature photoionization detector (miniPID) at four distances downstream of the odor source: (a) 50 mm, (b) 100 mm, (c) 200 mm and (d) 400 mm. Each trace is 15 s.

Fig. 7. Representative traces from the axial center of the continuous plume using a miniature photoionization detector (miniPID) at four distances downstream of the odor source: (a) 50 mm, (b) 100 mm, (c) 200 mm and (d) 400 mm. Each trace is 15 s.

Fig. 8. Conditional mean concentrations (± standard error) averaged over the center 12 mm by 12 mm core of each plume type relative to source concentration at four distances downstream of the odor source. The conditional mean is the mean formed during periods of active signal, rejecting regions of below-threshold signal.

Fig. 9. Intensity of concentration fluctuation (± standard error) estimated for each 'x' position from the linearized approximation to the relationship between mean concentration and standard deviation. Note that pulsed plumes do not vary much with downstream distance, but that continuous and oscillatory plumes have ratios that more than double downstream.

Fig. 10. Higher moments of concentration fluctuations: skewness and kurtosis of the oscillatory plume 100 mm downstream from the source. Values reported are from recordings at the plume's axial center, '0', moving outward toward the lateral edge.

Fig. 11. Intermittency values, $1-\gamma$, across the (a) continuous and (b) oscillatory plumes at two downstream distances, 50 and 400 mm, from the source. Values reported are from recordings at the plume's axial center, '0', moving outward toward the lateral edge.

Fig. 12. Intermittency values, $1-\gamma$, (± standard error) averaged over the center 12 mm by 12 mm core of each plume type at four distances downstream of the odor source.

Fig. 13. Peak-to-conditional-mean ratios (± standard error) of each plume type at four distances downstream of the source.

Fig. 14. Mean length of bursts (± standard error) recorded at the center 12 by 12 mm core of each plume type at four distances downstream of the odor source.

Fig. 15. Spectral density plots of the (a) vertical pulsed, (b and c) continuous, and (d and e) oscillatory plumes. Measurements were made at (a, b, and d) 100 mm and (c and e) 400 mm from the odor source. Peaks are evident at 10 Hz in the pulsed plume; the continuous and oscillatory plumes show several frequencies, and in both plume types, frequencies get larger with distance downstream.

6. Literature Cited

1. Mafra-Neto, A. and Cardé, R.T.: 1994, Fine-scale structure of pheromone plumes modulates upwind orientation of flying moths, *Nature*, **369,** 142-144.

2. Vickers, N.J. and Baker, T.C.: 1994, Reiterative responses to single strands of odor promote sustained upwind flight and odor source location by moths *Proc. Nat. Acad. Sci. U. S. A.*, **91,** 5756-5760.

3. Kennedy, J.S., Ludlow, A.R. and Sanders, C.J.: 1980, Guidance system used in moth sex attraction, *Nature*, **288**, 475-477.

4. Kennedy, J.S., Ludlow, A.R.and Sanders, C.J.: 1981, Guidance of flying male moths by wind-borne sex pheromone, *Physiol. Entomol.*, **6,** 395-412.

5. Geier, M., Bosch, O.J. and Boeckh, J.: 1999, Influence of odour plume structure on upwind flight of mosquitoes towards hosts, *J. Exp. Biol.*, **202,** 1639-1648.

6. Dekker, T., Takken, W. and Cardé, R.T.: 2001, Structure of host-odour plumes influences catch of *Anopheles gambiae s.s.* and *Aedes aegypti* in a dual-choice olfactometer, *Physiol. Entomol.*, **26,** 124-134.

7. Kennedy, J.S. and Marsh, D.: 1974, Pheromone-regulated anemotaxis in flying moths, *Science*, **184,** 999-1001.

8. Murlis, J. and Jones, C.D.: 1981, Fine-scale structure of odour plumes in relation to insect orientation to distant pheromone and other attractant sources. *Physiol. Entomol.*, **6**, 71-86.

9. Jones, C.D.: 1983, On the structure of instantaneous plumes in the atmosphere, *J. Hazard. Mater.*, **7**, 87-112.

10. Mylne, K.R. and Mason, P.J.: 1991, Concentration fluctuation measurements in a dispersing plume at a range of up to 1000 m, *Q.J.R. Meteorol. Soc.*, **117**, 177-206.

11. Yee, E., Chan, R., Kosteniuk, P.R., Chandler, G.M., Biltoft, C.A. and Bowers, J.F.: 1994, Experimental measurements of concentration fluctuations and scales in a dispersing plume in the atmospheric surface layer obtained using a very fast-response concentration detector. *J. Appl. Meteorol.*, **33,** 996-1016.

12. Fackrell, J.E. and Robins, A.G.: 1982, The effect of source size on concentration fluctuations in plumes. *Boundary-Layer Meteorol.*, **22**, 335-350.

13. Fackrell, J.E. and Robins, A.G.: 1982, Concentration fluctuations and fluxes in plumes from point sources in a turbulent boundary layer, *J. Fluid Mech.*, **117**: 1-26.

14. Mafra-Neto, A. and Cardé, R.T.: 1995, Influence of plume structure and pheromone concentration on upwind flight of *Cadra cautella* males, *Physiol. Entomol.*, **20,** 117-133.

15. Mafra-Neto, A. and Cardé, R.T.: 1995, Effect of the fine-scale structure of pheromone plumes: pulse frequency modulates activation and upwind flight of almond moth males. *Physiol. Entomol.,* **20**, 229-242.

16. Vickers, N.J. and Baker, T.C.: 1996, Latencies of behavioral response to interception of filaments of sex pheromone and clean air influence flight track shape in *Heliothis virescens* (F.) males, *J. Comp. Physiol. A.,* **178**, 831-847.

17. Vickers, N.J., Christensen, T.A., Baker, T.C. and Hildebrand, J.G.: 2001, Odour-plume dynamics influence the brain's olfactory code, *Nature,* **410**, 466-470.

18. Baker, T.C. and Linn, Jr., C.E. 1984, Wind tunnels in pheromone research. In: Techniques in pheromone research, H.E. Hummel & T.A. Miller (eds.), pp. 75-110, Springer-Verlag, New York.

19. Willis, M.A. and Baker, T.C.: 1994, Behaviour of flying oriental fruit moth males during approach to sex pheromone sources, *Physiol. Entomol.*, **19**, 61-69.

20. Cardé, R.T. and Knols, B.G.L.: 2000, Effects of light levels and plume structure on the orientation manoeuvres of male gypsy moths flying along pheromone plumes, *Physiol. Entomol.,* **25,** 141-150.

21. Justus, K.A., Schofield, S.W., Murlis, J. and Cardé, R.T.: 2002, Flight behaviour of *Cadra cautella* males in rapidly pulsed pheromone plumes. *Physiol. Entomol.* (in press).

22. Murlis, J. and Bettany, B.W.: 1977, Night flight towards a sex pheromone source by male *Spodoptera littoralis* (Boisd.) (Lepidoptera, Noctuidae). *Nature*, **268**, 433-435.

23. Murlis, J., Bettany, B.W., Kelley, J. and Martin, L.: 1982, The analysis of flight paths of male Egyptian cotton leafworm moths, *Spodoptera littoralis*, to a sex pheromone source in the field. *Physiol. Entomol.*, **7**, 435-441.

24. Christensen, T.A. and Hildebrand, J.G.: 1988, Frequency coding by central olfactory neurons in the sphinx moth *Manduca sexta*, *Chem. Senses*, **13,** 123-130.

25. Murlis, J., Willis, M.A. and Cardé, R.T.: 2000, Spatial and temporal structures of pheromone plumes in fields and forests, *Physiol. Entomol.,* **25**, 211-222.

26. Bartell, R.J.: 1982, Mechanisms of communication disruption by pheromone in the control of Lepidoptera: a review, *Physiol. Entomol.*, **7**, 353-364.

27. Vogel, S.: 1981, Life in Moving Fluids: The Physical Biology of Flow, Princeton University Press, 352 pp.

28. Willis, M.A., David, C.T., Murlis, J. and Cardé, R.T.: 1994, Effects of pheromone plume structure and visual stimuli on the pheromone-modulated upwind flight of male gypsy moths (*Lymantria dispar*) in a forest (Lepidoptera: Lymantriidae), *J. Insect Behav.,* **7,** 385-409.

29. Willis, M.A. and Baker, T.C.: 1984, Effects of intermittent and continuous pheromone stimulation on the flight behaviour of the oriental fruit moth, *Grapholita molesta*, *Physiol. Entomol.*, **9**, 341-358.

30. Weissburg, M.J., Dusenbery, D.B., Ishida, H., Janata, J., Keller, T., Roberts, P.J.W. and Webster, D.R.: 2002, A multidisciplinary study of spatial and temporal scales containing information in turbulent chemical plume tracking, *Environ. Fluid Mechanics*, (this issue).

31. Weissburg, M.J., Doall, M.H. and Yen, J.: 1998, Following the invisible trail: kinematic analysis of mate-tracking in the copepod *Temora longicornis*, *Phil. Trans. R. Soc. Lond B,* **353**, 701-712.

32. Willis, M.A., Murlis, J. and Cardé, R.T.: 1991, Pheromone-mediated upwind flight of male gypsy moths, *Lymantria dispar*, in a forest, *Physiol. Entomol.,* **16**, 507-521.

33. Atema, J.: 1996, Eddy chemotaxis and odor landscapes: exploration of nature with animal sensors, *Biol. Bull.,* **191,** 1129-138.

34. Webster, D.R. and Weissburg, M.J.: 2001, Chemosensory guidance cues in a turbulent chemical odor plume, *Limnol. Oceanogr.*, **46**, 1034-1047.

35. Marsh, D., Kennedy, J.S. and Ludlow, A.R.: 1978, An analysis of anemotactic zigzagging flight in male moths stimulated by pheromone, *Physiol. Entomol.*, **3**, 221-240.

	Pulsed plume	Continuous plume	Turbulent plume
mean track angle: (degrees ± SD)	53.5 ± 14.9	57.1 ± 12.5	42.0 ± 12.0
mean airspeed: (mm s^{-1} ± SD)	968 ± 107	947 ± 103	840 ± 68

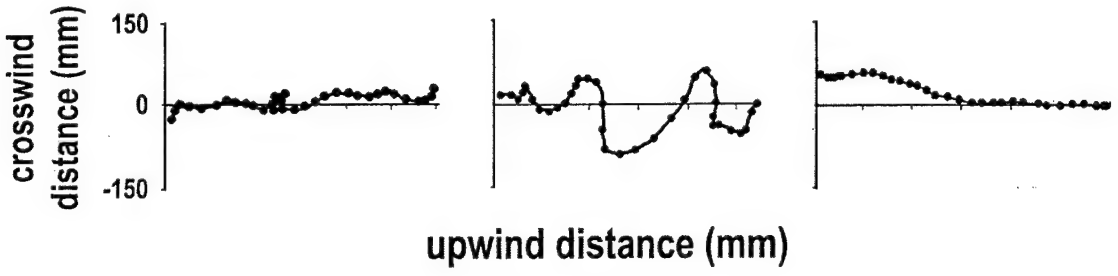

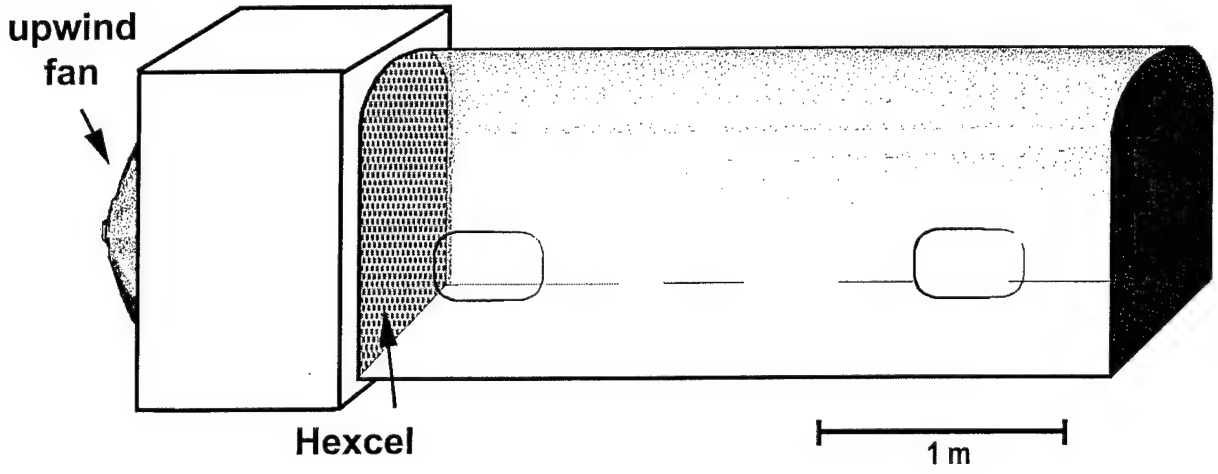
upwind
fan
Hexcel
1 m

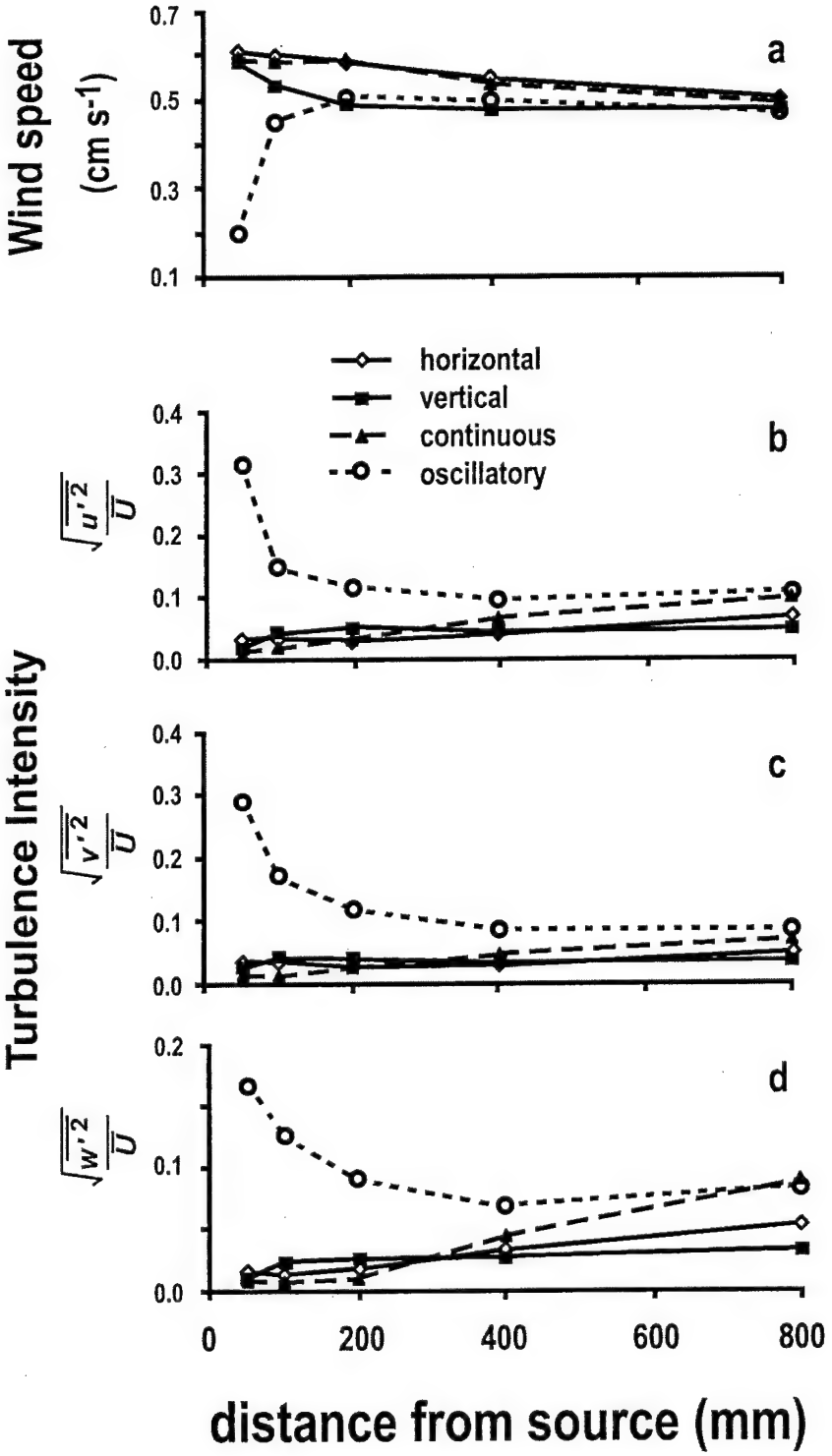
Wind speed
(cm s-1)
0.7
0.5
0.3
0.1
a
horizontal
vertical
continuous
oscillatory
b
c
d
Turbulence Intensity
0.4
0.3
0.2
0.1
0.0
0.2
0
200
400
600
800
distance from source (mm)

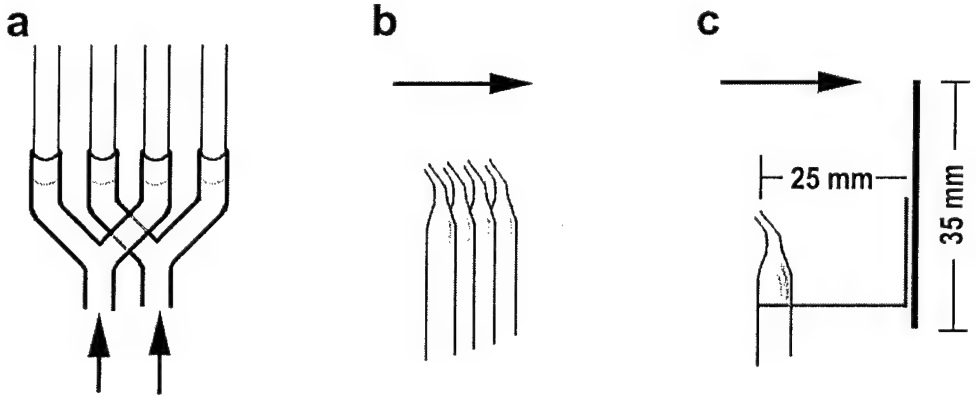
a
b
c
25 mm
35 mm

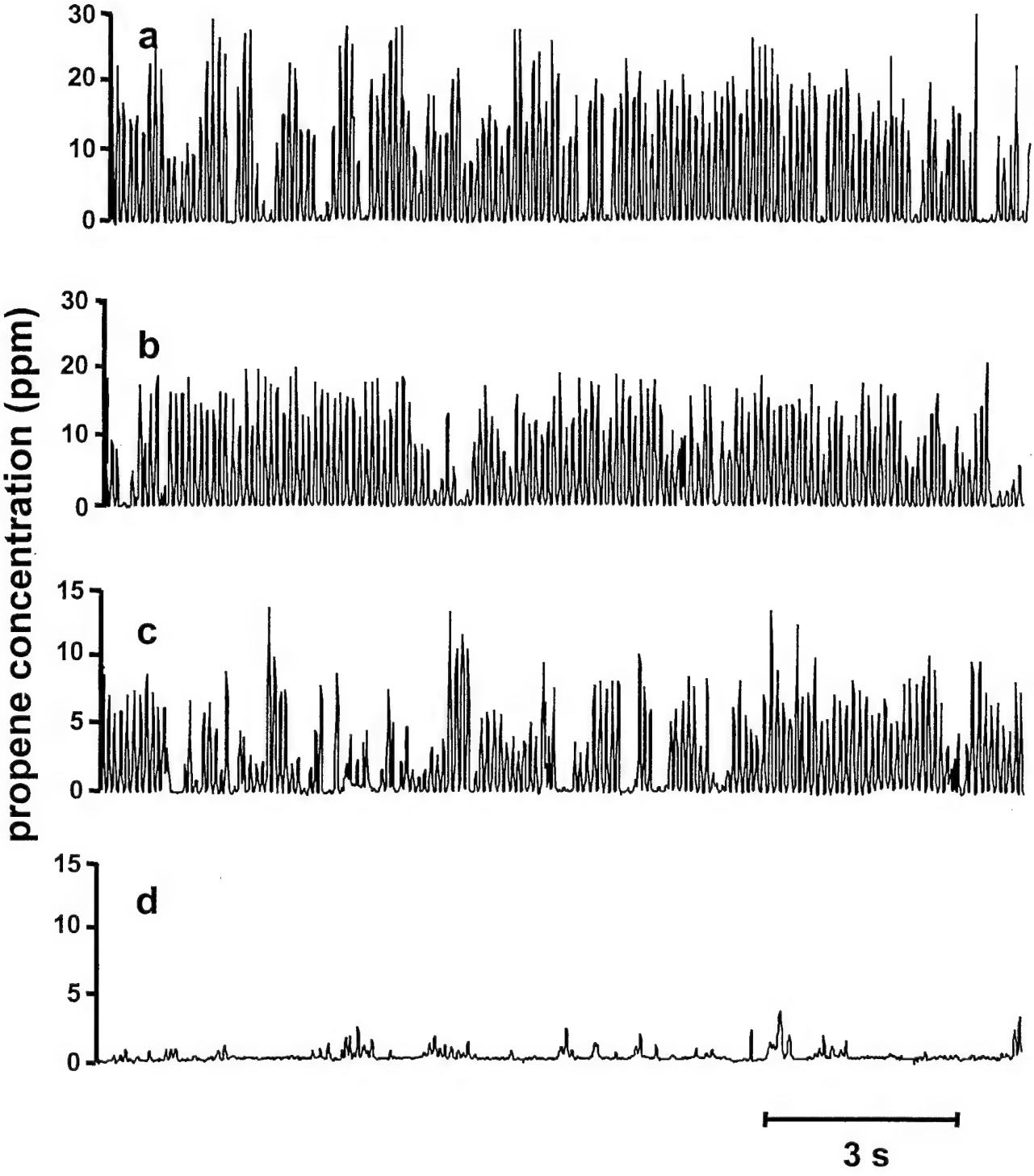
propene concentration (ppm)
a
b
c
d
30
20
10
0
30
20
10
0
15
10
5
0
15
10
5
0
3 s

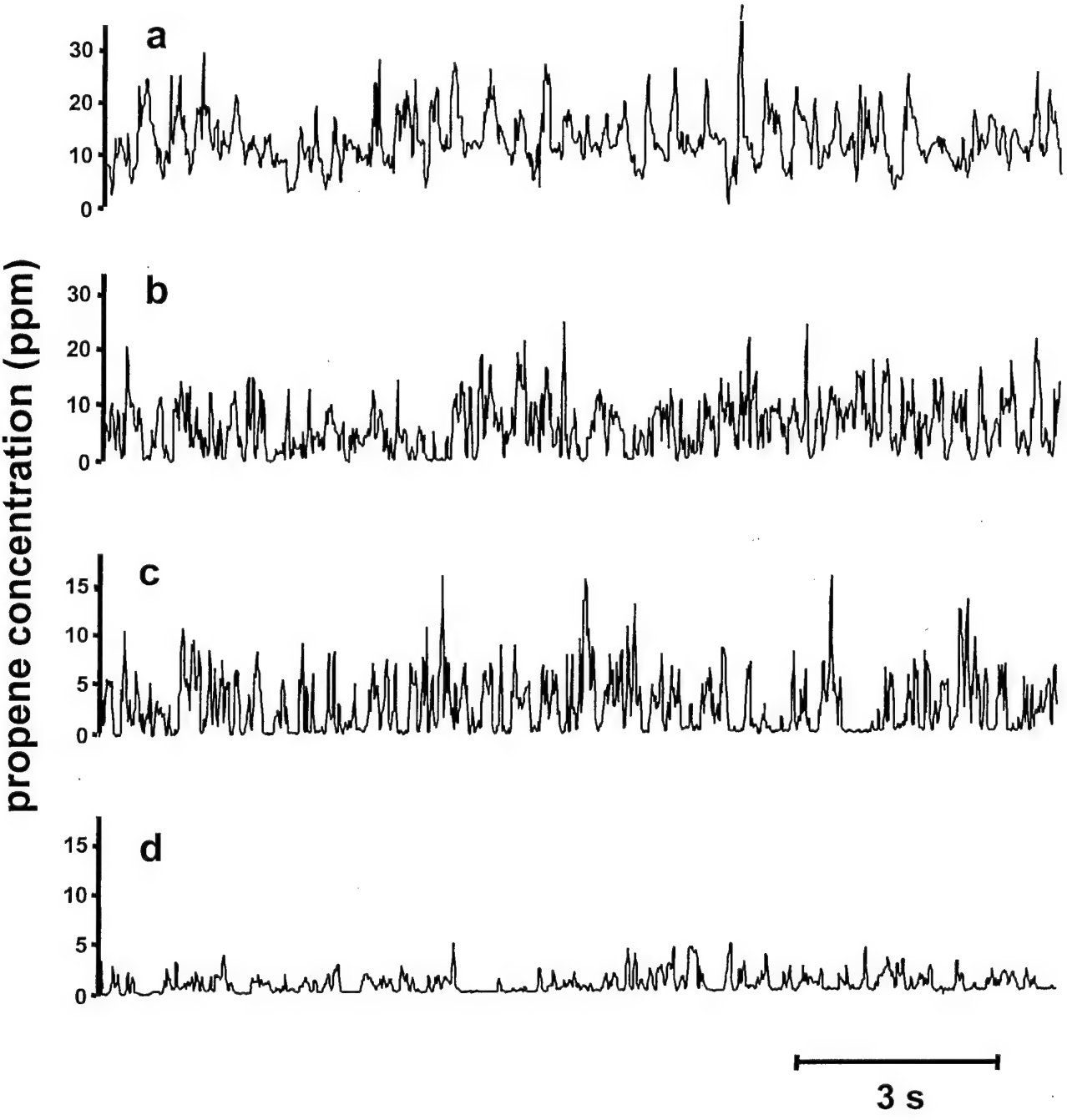
a
b
c
d
30
20
10
0
30
20
10
0
15
10
5
0
15
10
5
0
propene concentration (ppm)
3 s

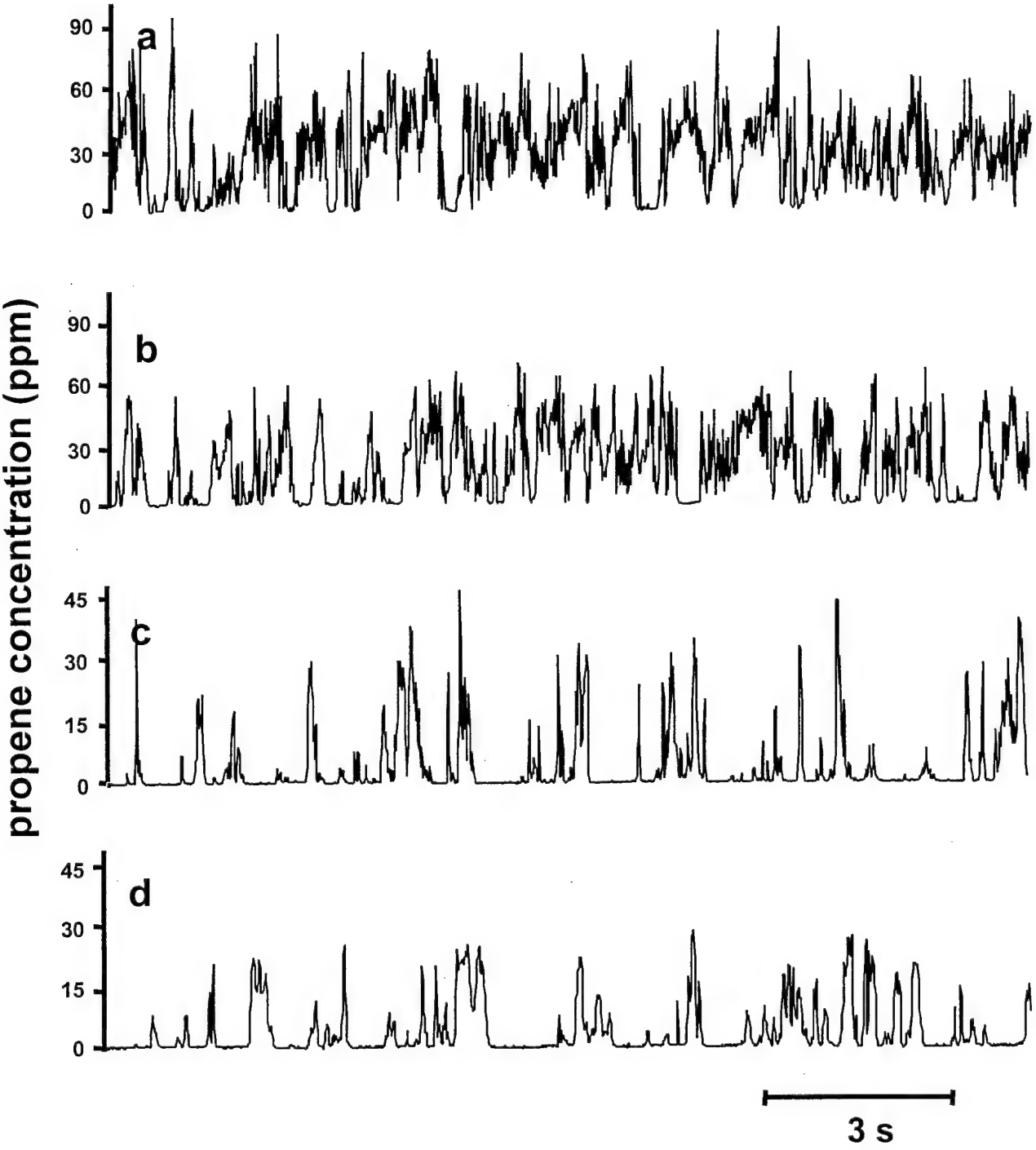
propene concentration (ppm)
a
b
c
d
90
60
30
0
90
60
30
0
45
30
15
0
45
30
15
0
3 s

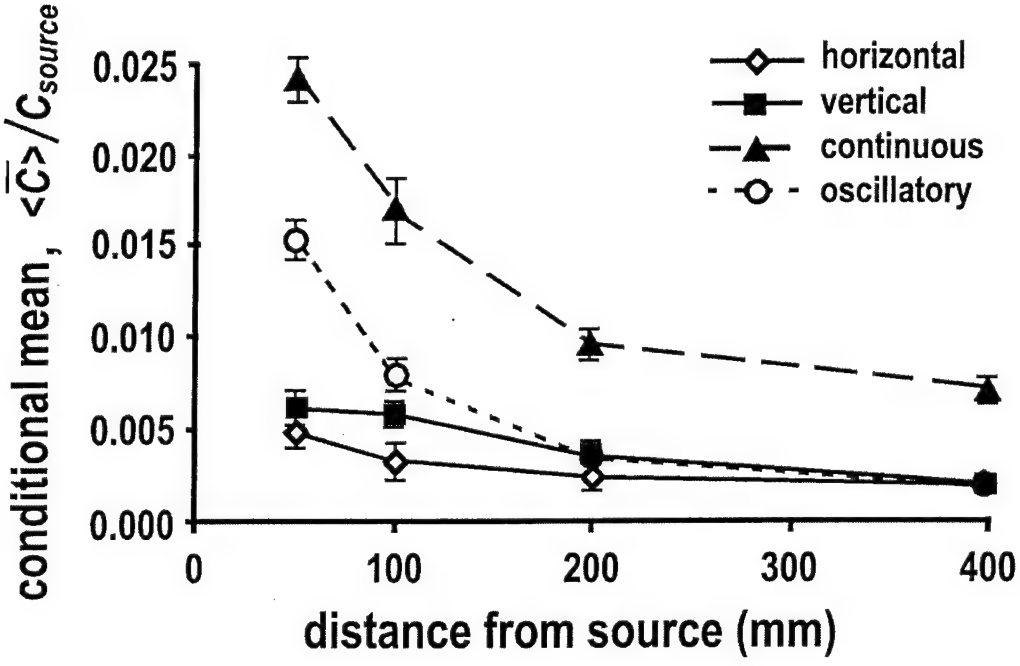
conditional mean, $\langle \bar{C} \rangle / C_{source}$
0.025
0.020
0.015
0.010
0.005
0.000
0
100
200
300
400
distance from source (mm)
horizontal
vertical
continuous
oscillatory

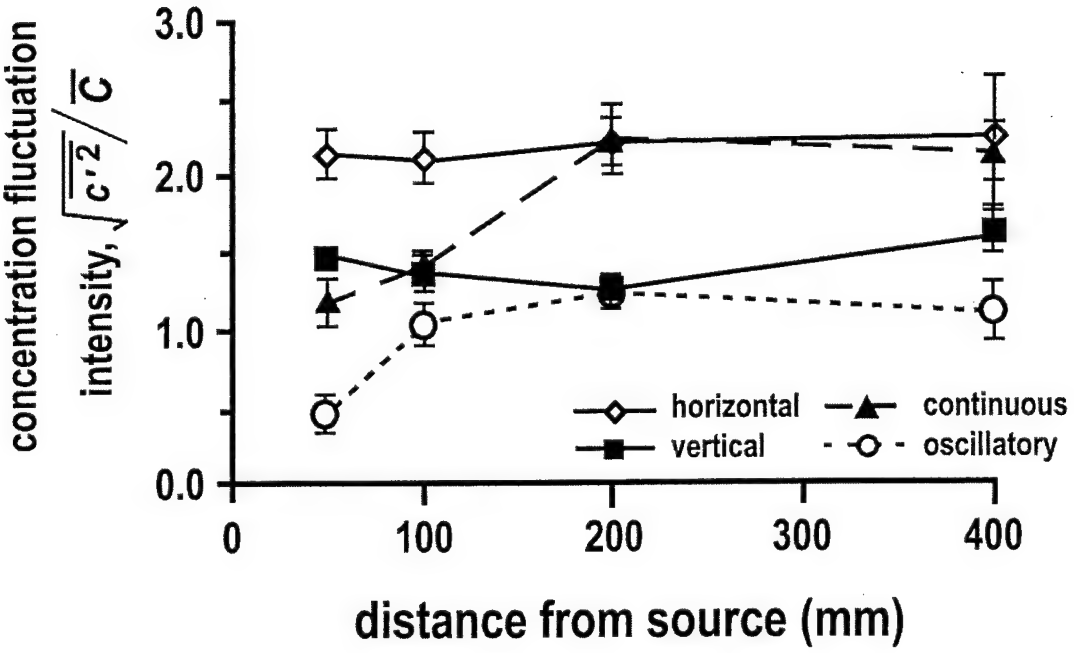
concentration fluctuation intensity, $\sqrt{\overline{c'^2}}/\overline{C}$
3.0
2.0
1.0
0.0
0
100
200
300
400
distance from source (mm)
horizontal
vertical
continuous
oscillatory

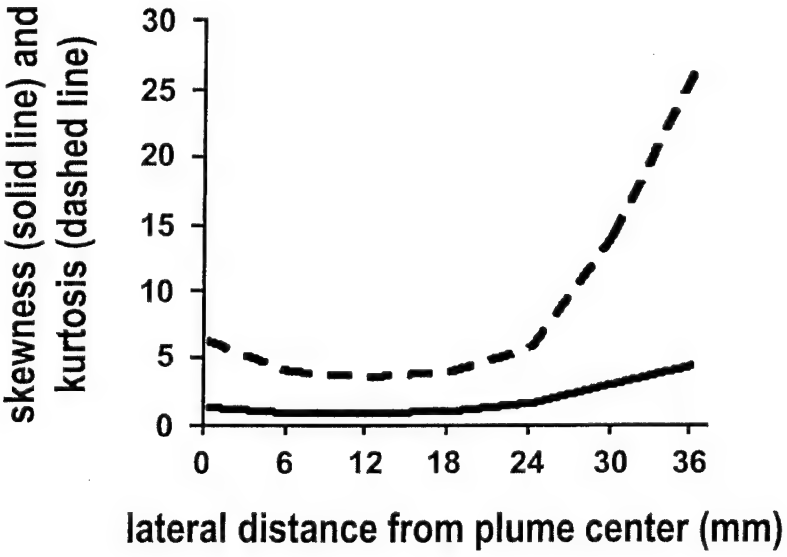
skewness (solid line) and
kurtosis (dashed line)
30
25
20
15
10
5
0
0
6
12
18
24
30
36
lateral distance from plume center (mm)

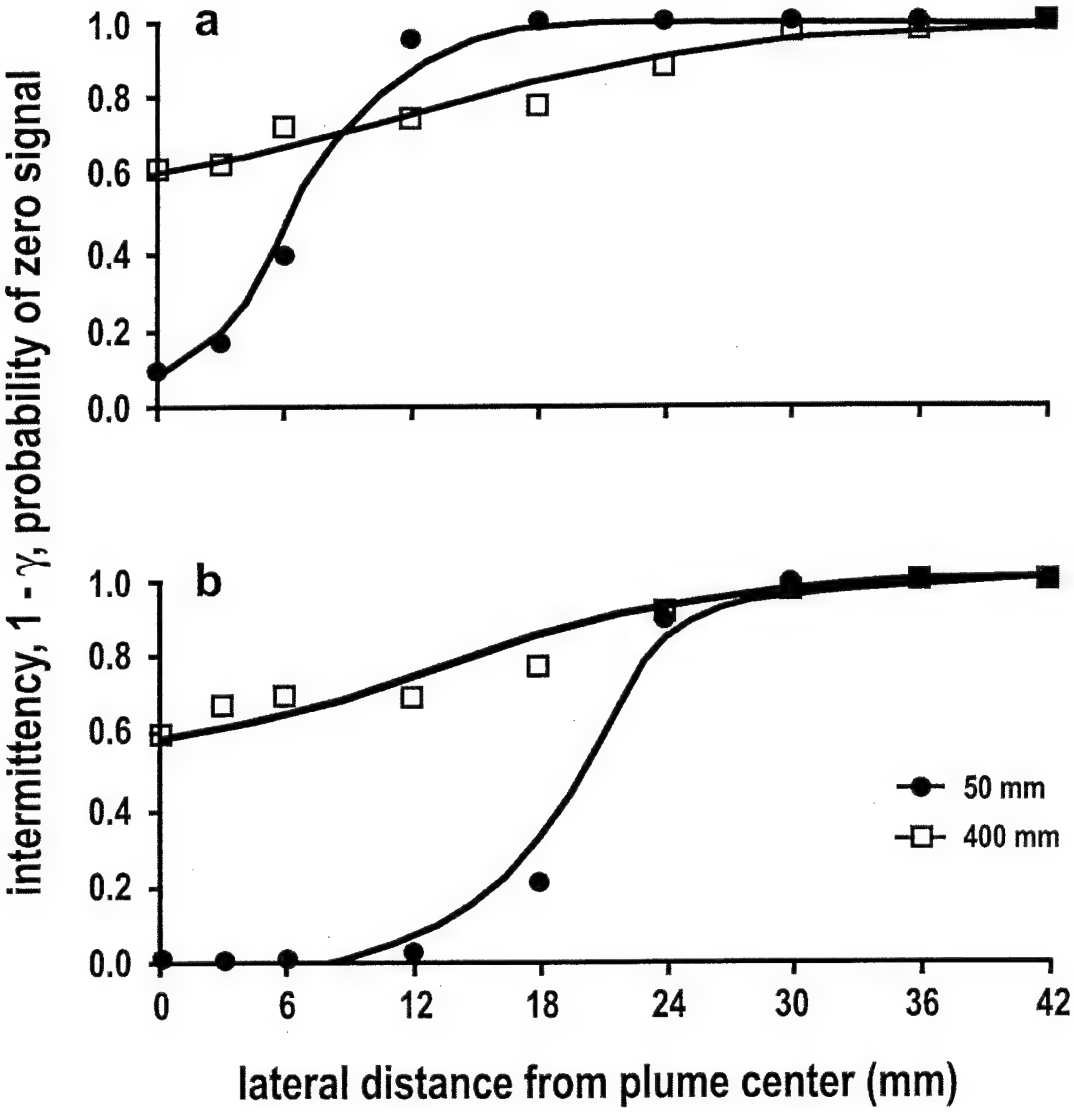
a
b
1.0
0.8
0.6
0.4
0.2
0.0
0
6
12
18
24
30
36
42
intermittency, 1 - γ, probability of zero signal
lateral distance from plume center (mm)
50 mm
400 mm

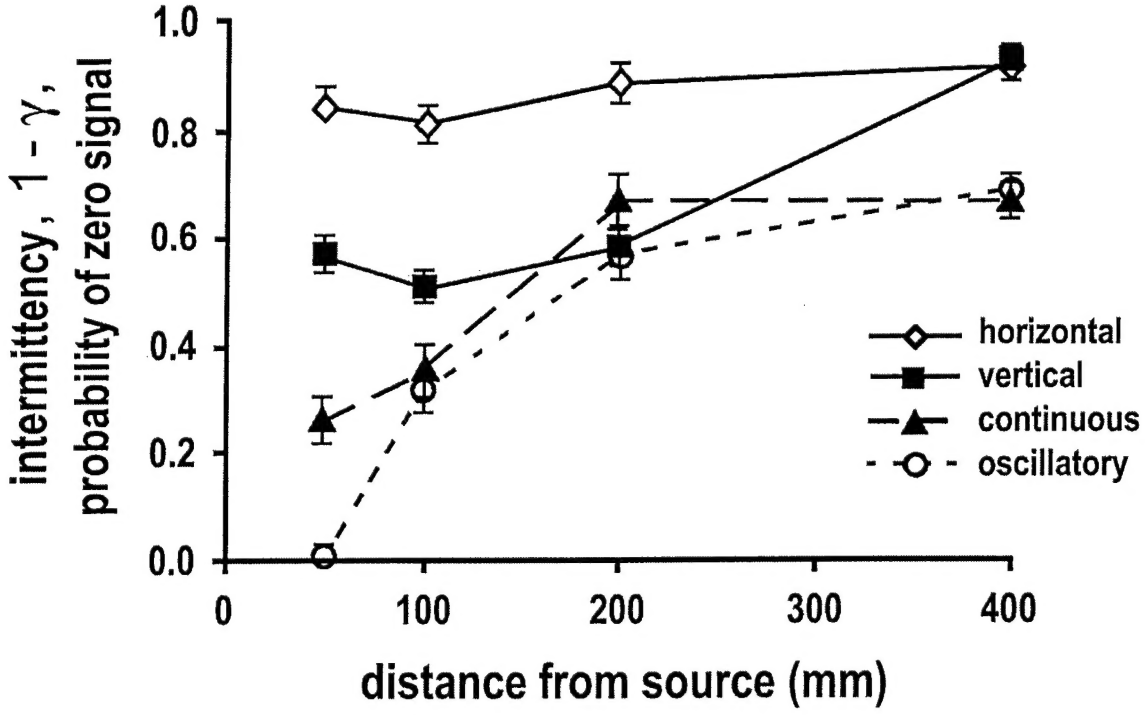
intermittency, 1 - γ,
probability of zero signal
1.0
0.8
0.6
0.4
0.2
0.0
0
100
200
300
400
distance from source (mm)
horizontal
vertical
continuous
oscillatory

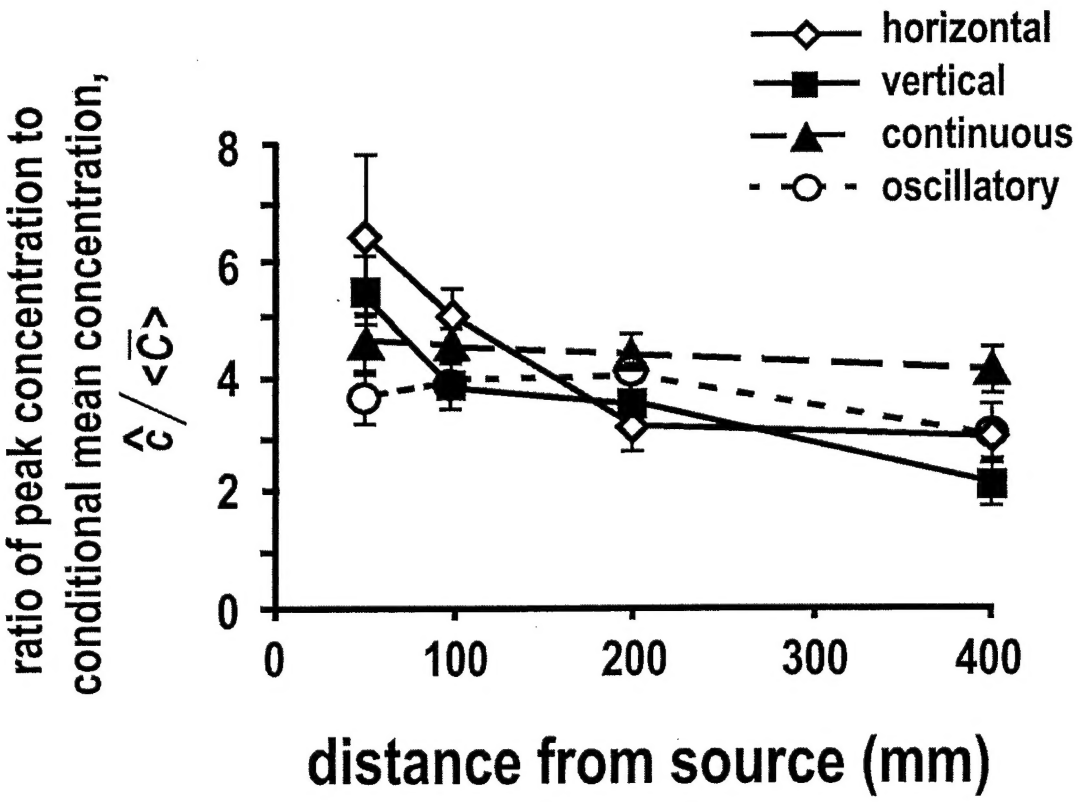
horizontal
vertical
continuous
oscillatory
ratio of peak concentration to conditional mean concentration, $\hat{c} / \langle \overline{C} \rangle$
0
2
4
6
8
0
100
200
300
400
distance from source (mm)

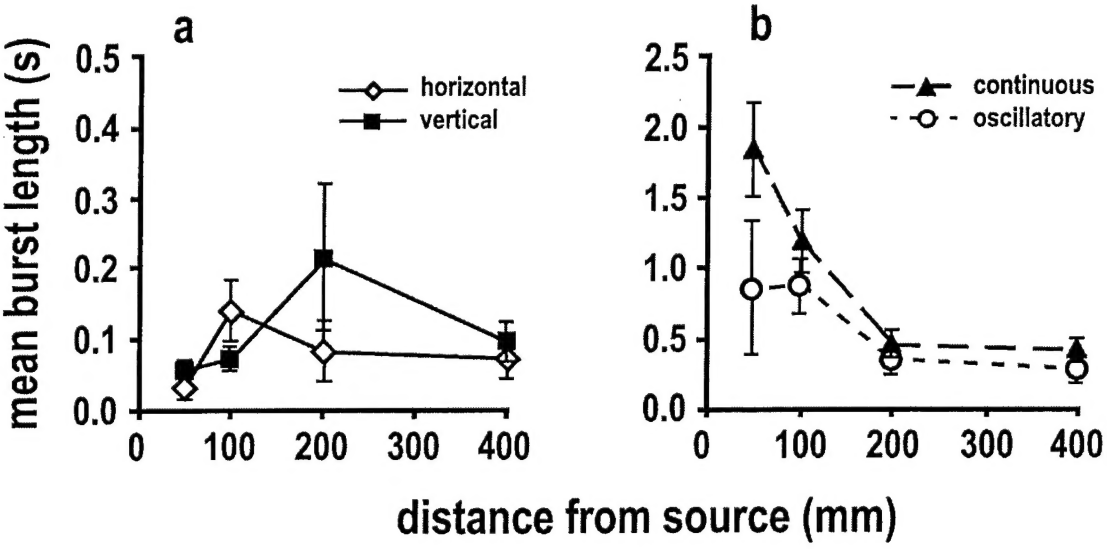
a
b
mean burst length (s)
0.5
0.4
0.3
0.2
0.1
0.0
horizontal
vertical
2.5
2.0
1.5
1.0
0.5
0.0
continuous
oscillatory
0
100
200
300
400
distance from source (mm)

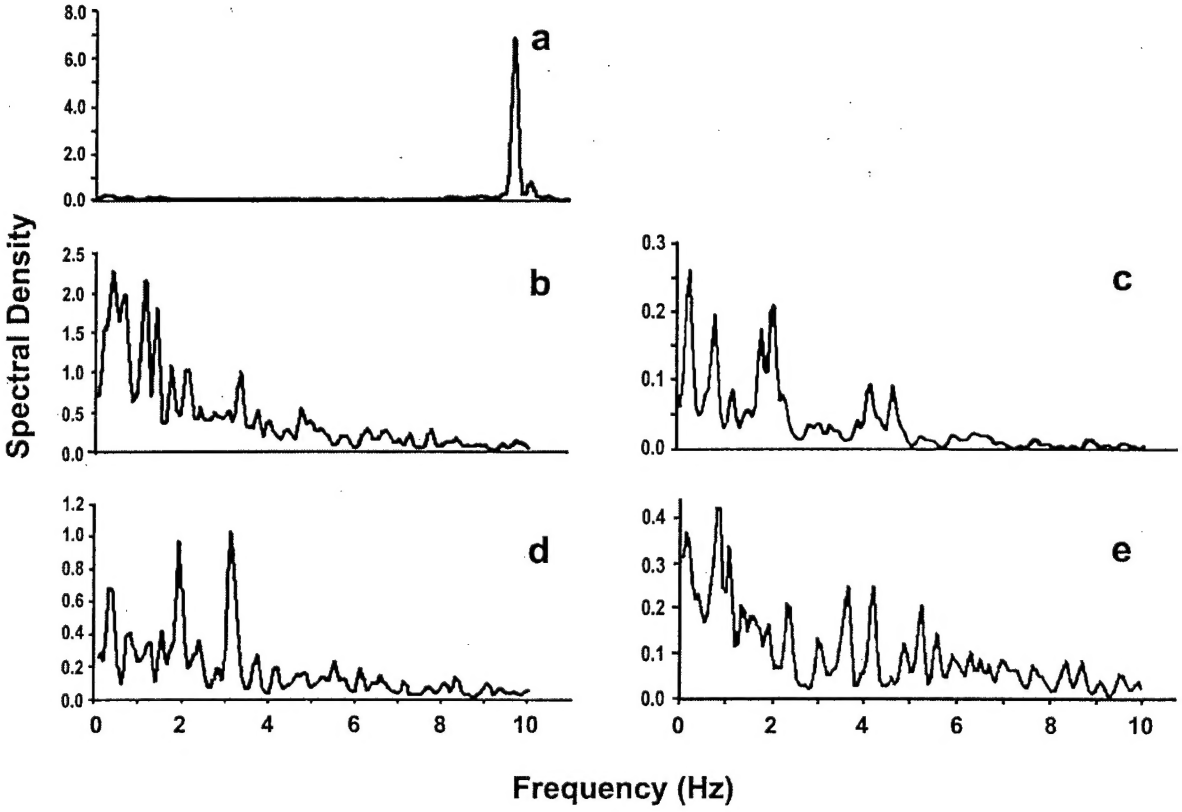
a
b
c
d
e
Spectral Density
Frequency (Hz)
8.0
6.0
4.0
2.0
0.0
2.5
2.0
1.5
1.0
0.5
0.0
0.3
0.2
0.1
0.0
1.2
1.0
0.8
0.6
0.4
0.2
0.0
0.4
0.3
0.2
0.1
0.0
0
2
4
6
8
10